공학석사학위논문

A Catalytic Hydrogel System Reinforced by Palladium Encapsulated Metal-Organic Framework for Suzuki-Miyaura Coupling Reaction

스즈키-미야우라 반응을 위한
팔라듐이 도입된 금속-유기 구조체로 강화한
하이드로젤 촉매

2018년 2월

서울대학교 대학원

재료공학부

조 성 인

Abstract

A Catalytic Hydrogel System Reinforced by Palladium Encapsulated Metal-Organic Framework for Suzuki-Miyaura Coupling Reaction

Seongin Jo
Department of Materials Science and Engineering
The Graduate School
Seoul National University

As environmental concerns increase, reactions in aqueous media are moving into the spotlight of synthetic chemistry where the usage of volatile organic solvents is reduced. We developed a catalytic hydrogel system for Suzuki-Miyaura coupling reaction in an aqueous medium. The hydrogel system contained palladium nanoparticle (PdNP) encapsulated metal-organic frameworks (MOFs) as catalytically active species and as reinforcement. The MOF (UiO-66-NH_2) was prepared from 2-aminoterephthalic acid and zirconium(IV) chloride. High surface area, chemical modifiability, and

numerous hydrogen bonding sites of UiO-66-NH_2 made it a good candidate for catalytic cage, chemical crosslinker, and physical filler, respectively. PdNPs were encapsulated inside of UiO-66-NH_2 by in situ hydrogen reduction and vinyl moieties for chemical crosslinking were introduced to UiO-66-NH_2 by postsynthetic modification. Palladium content and vinyl modification ratio were 2.79 and 96.1 %, respectively. No damage on the crystal structure of UiO-66-NH_2 was confirmed by nitrogen adsorption/desorption measurements and X-ray diffraction patterns. A catalytic hydrogel was prepared by free radical polymerization of acrylamide and the vinyl modified, PdNP encapsulated MOF in the presence of a small amount of a chemical cross-linker. The MOF reinforced hydrogel showed higher modulus and elongation by 105 and 25.8 %, respectively than the acrylamide hydrogel without the MOF. The catalytic activity and recyclability of the hydrogel were examined for the Suzuki-Miyaura coupling reaction of phenylboronic acid and iodobenzene.

.....

keywords **: hydrogel catalyst, heterogeneous catalyst, palladium nanoparticles metal-organic framework, Suzuki-Miyaura reaction, aqueous reaction**

Student Number **: 2016-20830**

Contents

1. Introduction

Recent topics in materials science are more focused on sustainable chemistry. Designing energy efficient process, using environmentally benign raw materials, and decreasing toxic byproducts are important considerations in sustainable chemistry, while performance, prices, and yields of the materials are primary concerns in traditional materials chemistry. The reduction of an organic solvent is particularly important since it produces over 80% of the waste in synthetic chemistry.[1] Petroleum-derived organic solvents produce pollutants during the whole cycle, from their generation to their disposal, either directly or indirectly. Water, an ideal solvent for sustainable chemistry, has been widely studied to replace organic solvents in whole or in part. Its abundancy and innocuousness make it attractive to chemists who care about environment, but problem is that most of the organic substances and the catalysts for synthetic reactions are insoluble in water.

Suzuki-Miyaura coupling reaction is one of the most powerful methods to build biaryl products by direct carbon-carbon bond formation. An aryl boronic acid reacts with an aryl halide or aryl triflate under basic conditions in the presence of a palladium catalyst. The reaction occurs throughout following three steps: oxidative addition, transmetalation, and reductive elimination (**Figure 1**).[2] In oxidative addition step, an aryl halide forms organopalladium complex with the catalyst, with corresponding oxidation of palladium from Pd(0) to Pd(II). Then nucleophilic carbon from an arylboronic acid is attached

to the complex by ligand transfer in transmetalation. Reductive elimination separates the product from the transmetalated complex, followed by reduction of the catalyst from Pd(II) to Pd(0). Mild reaction conditions, commercial viability, wide functional group compatibility, and flexibility in choosing a solvent make Suzuki-Miyaura coupling reaction valuable. Water or aquatic media are used as a solvent for the coupling reaction, in addition to various organic solvents like DMF and toluene. The reaction can be performed even in immiscible solvent systems like water/toluene with contact of reactant molecules at the interface.

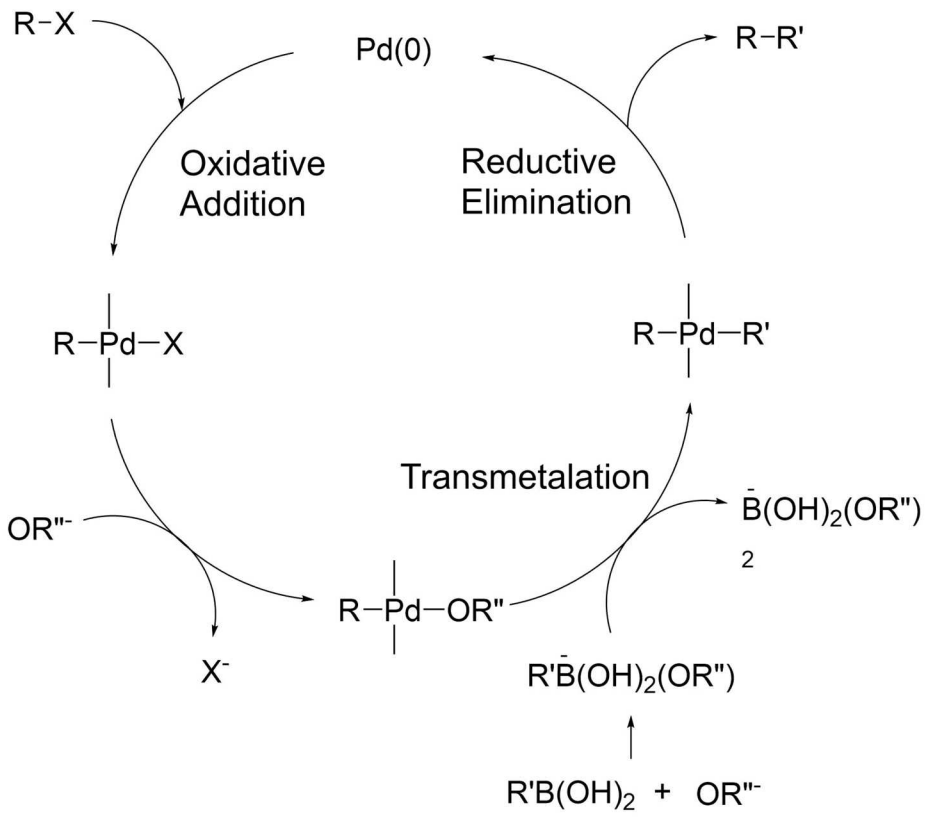

Figure 1 Mechanism of Suzuki-Miyaura coupling reaction.

Catalytic hydrogels are good candidates for sustainable catalysis in aqueous reactions because of their molecular versatility, chemical and physical stability, and hydrophilicity. The most common way to make a hydrogel to have catalytic ability is embedding metal nanoparticles (MNPs) within it. Butun et al. prepared poly(acrylamidoglycolic acid) hydrogels containing various metal nanoparticles such as silver, copper, nickel, and cobalt and successfully used

them for the reduction of 4-nitrophenol to 4-aminophenol.[3] Hydrogels with palladium nanoparticles were widely researched.[4–6] Lee et al. reported a poly(N-isopropylacrylamide-co-4-vinylpyridine) hydrogel which supported palladium nanoparticles. The hydrogel showed good catalytic ability in Suzuki-Miyaura coupling reaction, Heck-Mizoroki reaction, and Sonogashira coupling reaction in water.[4] Maity et al. introduced PdNPs into a calcium-cholate hydrid gel with simple blending of K_2PdCl_4, sodium cholate, and $Ca(NO_3)_2$ followed by reduction with cyanoborohydride.[5] Firouzabadi et al. proposed catalytic PdNP-agarose hydrogel system with good recyclability.[6]

The performance of a catalytic hydrogel system is dependent on not only content or activity of an embedded catalyst but also mechanical properties of a hydrogel matrix. A catalyst is exposed to harsh conditions during overall reaction processes including recycling procedures. Elevated temperature, vigorous stirring, extraction, washing, and drying processes can damage the hydrogel. Leakage of a poisonous and high-cost metal catalyst is a big problem in both environmental and economical views. Since most of MNP hydrogel catalyst systems in aforementioned researches were in powdery[3–5] or viscous gel-like[6] state, filtration and drying processes were required for recovery, consuming a lot of solvents and energy. The use of a bulk, monolithic, and tough catalytic hydrogel systems was expected to alleviate such problems.

Hydrogels can be reinforced by chemical crosslinkers or physical fillers. Chemical crosslinkers are organic compounds that have two or more functional groups, which form polymer networks *via* covalent bonding. Strong and permanent bonds developed by chemical crosslinkers make polymer networks

harder, leading to increment in mechanical properties and decrement in swelling property. Both modulus and elongation increase at low crosslink density, but after certain point, elasticity decreases and hydrogels become brittle. Physical crosslinkers interact with polymer chains *via* non-covalent way, such as ionic bonding, hydrogen bonding, coordination bonding, and hydrophobic interaction. Nanometer scale particle-type crosslinkers like nanoclay or silica nanoparticle are used for fillers. Secondary interactions between polymer chains and fillers are reversible, which are quite different from chemical bonds. If deformation larger than polymer chains can bear is applied to hydrogels, networks are reconstructured to have optimum structures (**Figure 2**).[7] On the other hand, tightly anchored polymer chains by chemical cross-linking cannot be rearranged by deformation. Physical crosslinking improves hydrogel's stretchability significantly, even at high filler concentrations up to 20 %.[8]

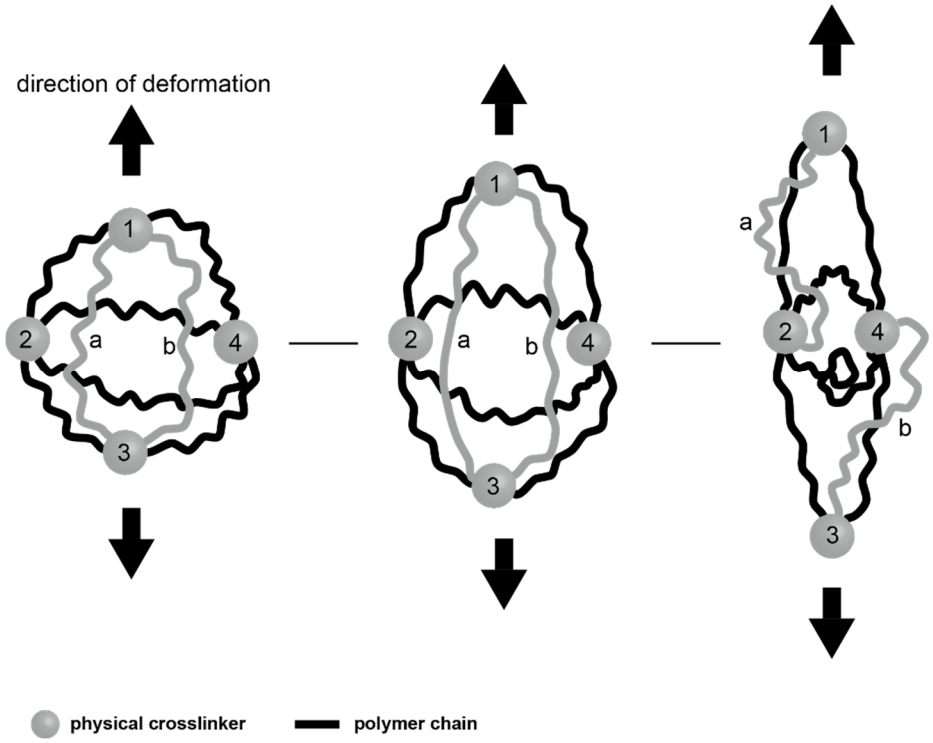

Figure 2 Change of a network structure while deformation in a physically crosslinked hydrogel. Grey colored polymer chains are rearranged. Chain (a) detached from linker 3 and reattached to linker 2 and chain (b) detached from linker 1 and reattached to linker 4.

A metal-organic framework (MOF) is a crystalline porous material consisting of metal nodes and organic linkers. A rigid network of the nodes and the linkers forms numerous micropores (pore diameter below 2 nm) and does not collapse after the removal of a solvent in synthetic process. Exceptionally high surface

areas and chemical, structural varieties are major advantages of MOFs in applications. They have been used for selective adsorption systems,[9,10] pollutant removal,[11] drug delivery,[12] and heterogeneous catalysts.[13,14]

Various molecular catalysts and MNPs have been introduced to MOFs because they can entrap guest catalysts both inside their pores and on their surfaces. A general method to introduce MNPs in MOFs is impregnation that is immersing MOFs in metal precursor solutions, followed by addition of reducing agents like sodium borohydride, ammonia borane or hydrogen. For example, PdNPs were introduced at UiO-66 by this method, and their catalytic ability was investigated in several studies.[15–17] Impregnation is a simple, easy method but most of MNPs formed by impregnation are located at the surface of an MOF, and there is a high possibility of particle aggregation. Recently, Liu et al. prepared UiO-66 with only interior platinum clusters by reducing a Pt precursor under hydrogen/air conditions.[18] The absence of external Pt clusters was confirmed by TEM and a size-selective catalytic reaction.

Postsynthetic modification (PSM) is a widely used technique to give MOFs more sophisticated functionalities. Organic linkers of MOFs can be easily modified without any damage to their crystal structures, which gives various advantages like higher selectivity to desired gas molecules,[19] granting catalytic activity,[20] and stimuli responsive pore size control.[21] The reaction between acyl chlorides[22,23] or organic acid anhydrides[24] and organic linkers with a modifiable functional group such as $–NH_2$ is used for PSM. The MOF's low processability due to its powder-like morphology and oleophobicity can be overcome by modification with polymerizable moieties or oleophilic molecules.

Zhang et al. constructed a flexible polymer-MOF membrane by introducing a polymerizable vinyl group to UiO-66-NH_2.[24] The MOF was uniformly dispersed throughout the resulting membrane and its microporous structure was not disturbed.

A stable mixed-matrix membrane can also be prepared by hydrogen bonding between an MOF particle and a polymer chain without chemical modification. Un-coordinated ligand groups such as carboxyl, pyridine, and imidazole groups can act as hydrogen bonding sites in a –OH or –NH rich polymer membrane. Zhang et al. fabricated a pervaporation membrane with MIL-53 and PDMS by hydrogen bonding between polydimethylsiloxane and MIL-53 particles.[25] Feijani et al. prepared a mixed matrix membrane with MIL-53 and poly(vinylidene fluoride), which showed improved CO_2/CH_4 separation properties.[26] Shen et al. reported that the polymer-MOF interaction could be enhanced by introducing $–NH_2$ group on ligand by PSM.[27]

Considering all the factors mentioned above, a hydrogel system with MNP-containing MOFs can be a stable and sustainable catalyst for a reaction in an aqueous medium. MNPs encapsulated in an MOF are more stable during the catalytic cycles than free MNPs. Chemical or physical bonding between an MOF and hydrogel backbones can be constructed by the PSM method or by hydrogen bonding. These chemical bonding and physical interactions can reinforce a hydrogel, resulting in a more stable catalytic system. An MOF particle can act as a catalyst cage, chemical crosslinker, and physical filler simultaneously. There have been a few studies about incorporating MOFs into hydrogels,[28–31] but none of them reported such a multi-functional MOF.

In this work, we prepared a new catalytic hydrogel system reinforced by palladium encapsulated MOFs. UiO-66-NH_2 was chosen as an MOF because it is stable in water even at elevated temperatures and at a wide range of pH,[32] which makes it suitable for Suzuki-Miyaura coupling reaction, as the reaction performs in basic aqueous media. Palladium nanoparticles were introduced by in-situ hydrogen reduction method (Pd@UiO-66-NH_2), and the resulting MOF was modified with acryloyl chloride to have vinyl functionality (Pd@UiO-66-acr). The encapsulation of Pd nanoparticles was confirmed by transmission electron microscopy (TEM) and energy-dispersive X-ray spectroscopy (EDS). The vinyl group modification was confirmed by nuclear magnetic resonance (NMR) spectroscopy and X-ray diffraction (XRD) analysis. The acrylamide hydrogel was synthesized with a modified Pd containing MOF. Uniformly dispersed MOF clusters were observed by scanning electron microscopy (SEM). The overall fabrication process is summarized in **Figure 3**. Catalytic ability of the hydrogel system was evaluated by performing Suzuki-Miyaura coupling reaction in ethanol/water.

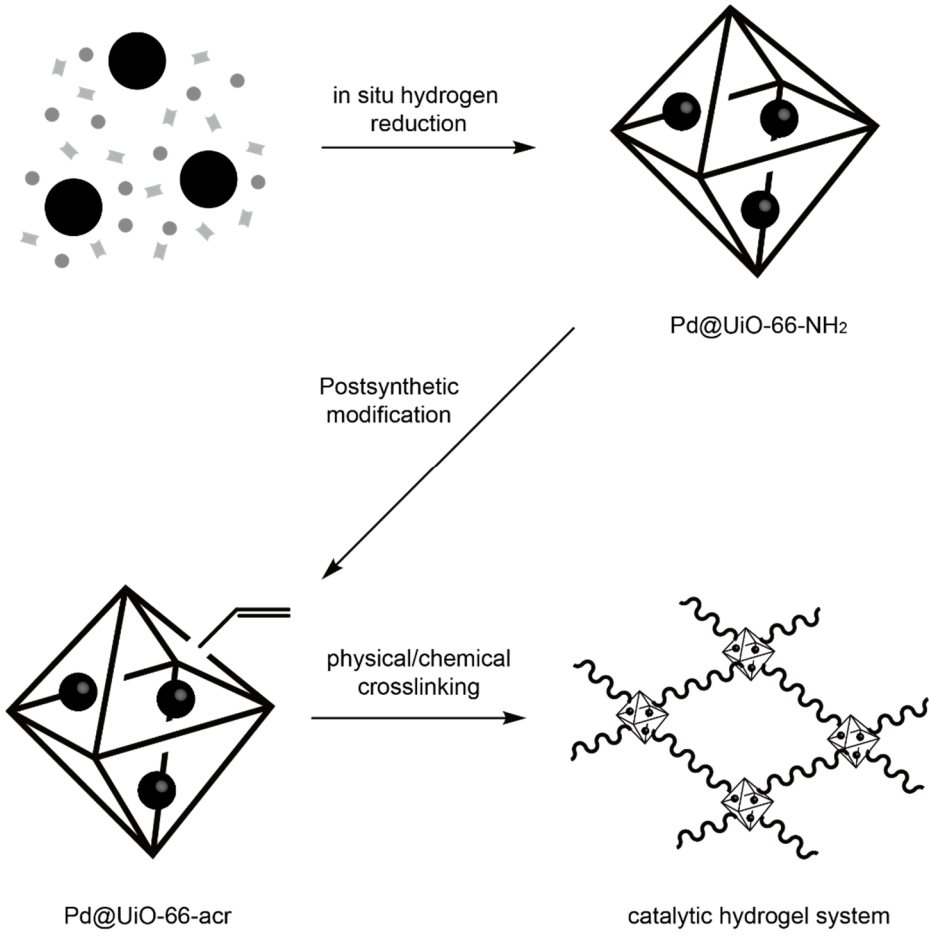

Figure 3 Schematic representation of overall fabrication process.

2. Experimental

2.1. Materials

Zirconium(IV) chloride and potassium persurfate (KPS) were purchased from Acros Organics. Palladium(II) acetate, tetramethylethylenediamine (TEMED), N,N'-methylenebisacrylamide (MBAA) and iodobenzene were purchased from Sigma Aldrich. 2-aminoterephthalic acid was purchased from Alfa Aesar. Phenylboronic acid, acrylamide (AAm), and acryloyl chloride were purchased from Tokyo Chemical Industry. Potassium carbonate (K_2CO_3) was purchased from Daejung Chemical & Metals. Hydrofluric acid was purchased from J.T. Baker. N,N-dimethylformamide (DMF), n-hexane, ethyl acetate, ethanol, acetic acid, and tetrahydrofuran (THF) were purchased from Junsei and used without further purification. THF was dehydrated with sodium before use.

2.2. Synthesis of UiO-66-NH_2

UiO-66-NH_2 and Pd@UiO-66-NH_2 was prepared according to the reported literature.[18] 2-aminoterephthalic acid (200 mg, 1.10 mmol) and zirconium(IV) chloride (233.4 mg, 1 mmol) were dissolved in N,N-dimethylformamide (80 ml). Acetic acid (0.66 ml, 20 eq. to $ZrCl_4$) was added to the solution as a modulator. After 20 min of sonication, the reaction solution was heated to 120 ℃ and kept for 24 h with vigorous stirring. Resulting yellowish powder was

collected by filtration with a 0.2 μm PTFE membrane filter and washed with DMF (60 ml, 3 times) and ethanol (60 ml, 3 times). UiO-66-NH_2 was dried in vacuum oven at 120 ℃ for 24 h before use.

2.3. Synthesis of Pd@UiO-66-NH_2

Aforementioned in-situ hydrogen reduction method was used to synthesize Pd nanoparticle encapsulated MOF, Pd@UiO-66-NH_2. 2-aminoterephthalic acid (200 mg, 1.10 mmol), zirconium(IV) chloride (233.4 mg, 1 mmol), and palladium(II) acetate (20 mg, 0.089 mmol) were dissolved in N,N-dimethylformamide (80 ml). Acetic acid (2.97 ml, 90 eq. to $ZrCl_4$) was added to the solution as a modulator. After 20 min of sonication, the reaction solution was heated to 120 ℃ with vigorous stirring. Hydrogen gas was injected 1 h after the solution reached at 120 ℃ to maintain proper formation speed of MOF and Pd nanoparticles. Resulting grey powder was collected by filtration with a 0.2 μm PTFE membrane filter and washed with DMF (60 ml, 3 times) and ethanol (60 ml, 3 times). Pd@UiO-66-NH_2 was dried in vacuum oven at 120 ℃ for 24 h before use.

To make Pd encapsulated UiO-66-NH_2 by impregnation, dried MOF (100 mg) was dispersed in palladium(II) acetate solution in THF (20 ml, 3 mg/ml) by 20 min of sonication. After 2 h of vigorous stirring in room temperature, resulting brown powder was collected by membrane filter and washed with THF (30 ml, 3 times) and ethanol (30 ml, 3 times). Collected MOF was dried in vacuum oven at 80 ℃ then palladium(II) was reduced with sodium

borohydride solution in water (2 ml, 2.4 mg/ml). Resulting black powder was isolated with same filtration and washing process with above.

2.4. Postsynthetic modification of Pd@UiO-66-NH_2

Dried Pd@UiO-66-NH_2 (200 mg) was dispersed into dry THF (30 ml) by 10 min of sonication. After adding acryloyl chloride (0.12 ml, 2.5 eq. to $–NH_2$), the solution was kept at room temperature for 48 h with vigorous stirring. Resulting grey powder was collected by membrane filter and washed with THF (60 ml, 3 times) and ethanol (60 ml, 3 times). Pd@UiO-66-acr was dried in vacuum oven at 120 ℃ for 24 h before use.

2.5. Fabrication of catalytic hydrogel system

Acrylamide (600 mg, 8 wt% to water) was dissolved in deionized water (7.5 ml). For MOF nanocomposite gels, Pd@UiO-66-NH_2 or Pd@UiO-66-acr (90 mg, for unmod-gel and mod-gel respectively) were added. After 30 min of sonication, potassium persurfate (3 mg, 0.5 wt% to acrylamide), N,N'-methylenebisacrylamide (3 mg, 0.5 wt% to acrylamide), and tetramethylethylenediamine (15 μl) were added to solution. Hydrogels were fabricated by free radical polymerization in 40 ℃ for 3 h. All gels were used as-spun for tensile test and mod-gel was soaked into deionized water for 24 h to remove unreacted monomer for catalytic reaction.

2.6. Suzuki-Miyaura coupling reaction

Phenylboronic acid (36.6 mg, 0.3 mmol), iodobenzene (27.9 μl, 0.25 mmol), and potassium carbonate (69.1 mg, 0.5 mmol) were dissolved in 1:1 EtOH/water solution (2 ml). After adding the catalyst (750 mg), reaction was taken for 24 h in 60 ℃ with stirring. Reaction solution was diluted with water (10 ml) and extracted with ethyl acetate (10 ml, 3 times). The organic phase was separated and evaporated for isolation of product. For recycling test, the catalytic hydrogel was immersed in ethyl acetate and water for 24 h respectively.

2.7. Characterization

2.7.1. Nuclear magnetic resonance spectroscopy

^{1}H-NMR spectra were recorded by 300 MHz Bruker Avance DPX-300 spectrometer using d_6-DMSO as a solvent. All chemical shifts were calculated from tetramethylsilane. Spectra of modified and unmodified MOF were obtained from the digested sample of Pd@UiO-66-NH_2 and Pd@UiO-66-acr (10 mg) with HF (550 μl) in d_6-DMSO (550 μl).

2.7.2. N_2 adsorption/desorption measurements

N_2 adsorption/desorption measurements were performed by Belsorp-Max (BEL Japan, Inc.) equipment at 77 K. Pore size distributions were obtained by applying the non-local density functional theory (NLDFT).

2.7.3. X-ray diffraction measurements

Powder X-ray diffraction patterns were obtained by Bruker New-D8 Advance, with Cu Kα source (λ = 1.54 Å). Source voltage and current were set to 40 kV and 40 mA, respectively.

2.7.4. Scanning electron microscopy

Scanning electron microscopy (SEM) images were obtained by Carl Zeiss SUPRA 55VP. All samples were coated with platinum before the measurement. Energy dispersive X-ray spectroscopy (EDS) was performed and analyzed with Oxford instrument X-MaxN detector and AZtecEnergy EDS analyzer. The MOF sample for EDS measurement was carried out without platinum coating to avoid miscalculation occurred by signal range overlap of zirconium and platinum.

2.7.5. Transmission electron microscopy

Transmission electron microscopy (TEM) images were obtained by Talos L120C at 120kV. MOF samples were dispersed in ethanol and dropped on a carbon coated copper TEM grid.

2.7.6. Tensile test

Tensile test was performed by Instron-5543 Universal Testing Machine (UTM). Load and test speed were set to 1 kN and 1 cm/min, respectively. Test samples were cut into a rectangular sheet (1 mm x 1 cm x 4 cm) with a laser cutter. Top 1.5 cm and bottom 1.5 cm of the samples were fixed to apparatus, and the final sample length was configured to 1 cm.

3. Result and Discussion

3.1. Synthesis of UiO-66-NH_2 and Pd@UiO-66-NH_2

UiO-66-NH_2 and Pd@UiO-66-NH_2 were synthesized by solvethermal reaction of $ZrCl_4$ and 2-aminoterephthalicacid with acetic acid as a modulator in DMF. Palladium(II) acetate and hydrogen gas were used as a precursor and a reducing agent, respectively. Dispersivity of a MOF in water is the most important factor in the fabrication of a MOF-hydrogel composite. UiO-66-NH_2 had a lot of hydrogen bonding sites on its surface, and showed very strong hydrophilicity. But those hydrogen bonding sites also made MOF particles to form aggregated clusters,[33] and therefore decreasing cluster size was more important than decreasing the size of each MOF particle.

A modulator is a one-site ligand that coordinates with metal clusters in a MOF precursor solution to disturb the bonding of the clusters and linkers. An exchange of coordinated modulator molecules on the clusters with desired organic linkers should be occurred to construct the MOF crystal. It is different from the un-modulated MOF synthesis that organic linkers coordinate with metal-oxo cluster freely to form nuclei. This disturbance by the modulator can decrease the total MOF nuclei number and fewer nuclei make MOF crystals to grow larger.[34] Overall mechanisms of the modulated and un-modulated MOF synthesis are shown in **Figure 4**. The surface to volume ratio of a crystal decreases when the crystal size increases. The optimum modulator

concentration for the Pd@UiO-66-NH_2 synthesis was found to be 90 eq. to $ZrCl_4$.

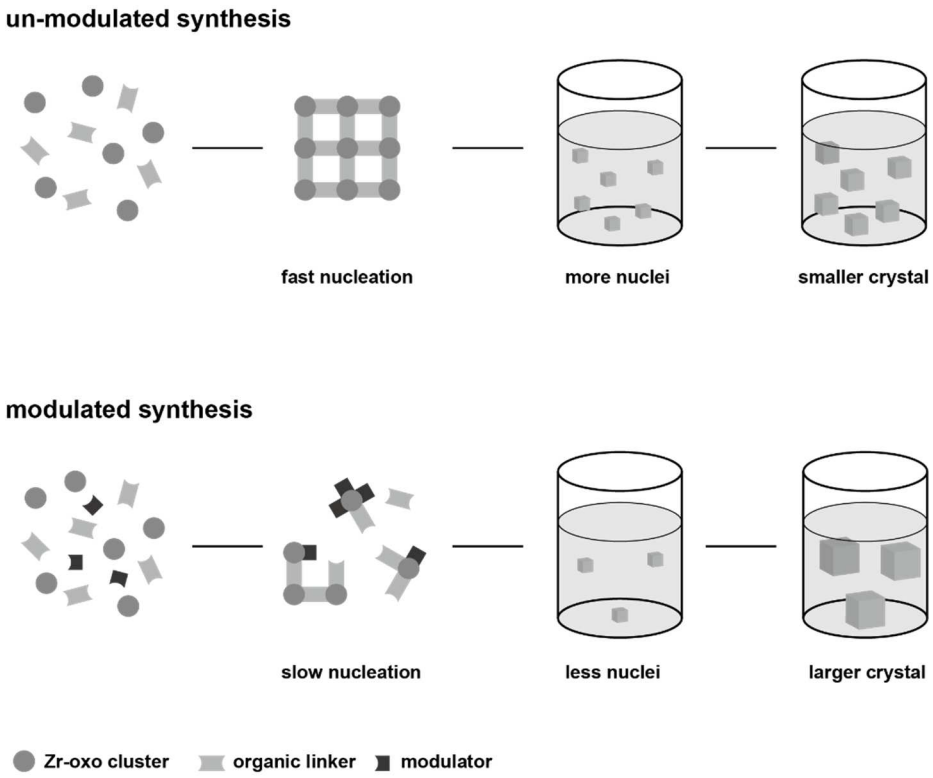

Figure 4 Mechanisms for the un-modulated and modulated synthesis of MOF.

An in-situ hydrogen reduction method used in this research is a technique that has been used for the growth of a MOF crystal on a metal nanoparticle. The high surface energy of a nano-sized palladium particle makes monomers of the

MOF to surround the nanoparticle, similar to the heterogeneous nucleation process. The growth of the MOF occurs on the palladium nanoparticle seeds and PdNPs that contain growing MOF units form large crystals with a lot of encapsulated nanoparticles. PdNPs can be introduced “inside” of the MOF, which is the most powerful advantage of the method. Impregnation is not suitable for the encapsulation of nanoparticles, especially in small-pore MOFs like a UiO-66 family. Since a small pore window diameter makes the permeation of a metal precursor and reducing agent solution difficult, the nanoparticle formation inside the pore becomes unfavorable. Differences between two nanoparticle introducing methods are shown in **Figure 5**. The MOF formation and nanoparticle fabrication speed must be adjusted for the successful heterogeneous nucleation by palladium nanoparticles. Pre-constructed nanoparticles were aggregated and separated from MOF crystals when hydrogen gas was injected from the beginning, due to the slow MOF growth speed in the modulated synthesis. In the optimized modulator concentration, the reaction bath was exposed to hydrogen gas for 1 h after reaching to the reaction temperature and the PdNP encapsulating MOF was successfully synthesized.

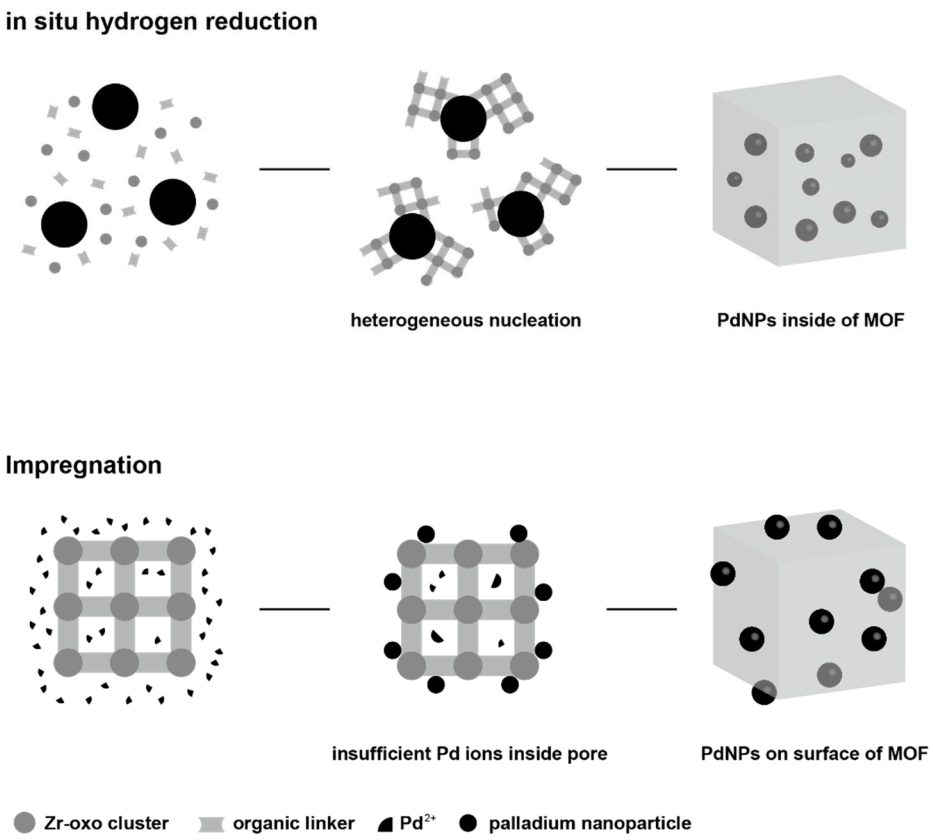

Figure 5 Comparison of PdNP introducing mechanisms for in situ hydrogen reduction and impregnation.

3.2. Characterization of the MOF

Synthesized UiO-66-NH_2 and Pd@UiO-66-NH_2 were characterized with nitrogen adsorption/desorption measurements, X-ray diffraction, scanning electron microscopy, and transmission electron microscopy.

Nitrogen adsorption/desorption measurement results are shown in **Figure 6**. Adsorption/desorption isotherms of UiO-66-NH_2 and Pd@UiO-66-NH_2 exhibited type I profiles which are found at microporous materials. BET surface areas of UiO-66-NH_2 and Pd@UiO-66-NH_2 were 1387 m^2/g and 978 m^2/g, respectively. According to Liu et al. the formation of an MOF crystal is followed by two steps, explosive nucleation and aggregation, and the growth of the small nuclei.[35] With high concentration of monomers, fast nucleation occurs until the solute level is below the critical nucleation point. Small nuclei aggregate to lower the surface energy after the nucleation stops and the slow growth process occurs. Therefore, the inner layer of the MOF crystal has more defects and the outer shell has a more robust structure. Compared to the homogeneous nucleation, the heterogeneous nucleation process has a faster nucleation speed and causes the crystal mismatch between the MOF and PdNP. These phenomena lead to the increment of disorientation in the aggregate interface, making MOF crystals to have more defects inside. UiO-66-NH_2 and Pd@UiO-66-NH_2 had the same pore diameters of 0.86 nm obtained from the NLDFT pore size distribution analysis, which were similar to the reported data of the UiO-66 family.[18]

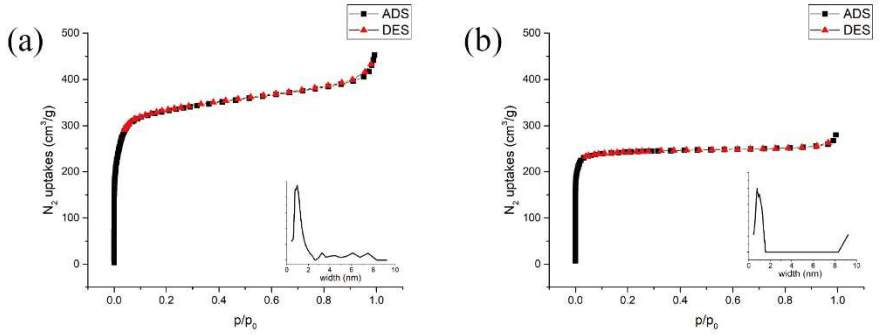

Figure 6 N_2 adsorption/desorption isotherms for (a) UiO-66-NH_2 and (b) Pd@UiO-66-NH_2. Inset graphs are NLDFT pore size distributions.

Figure 7 shows SEM and TEM images of Pd@UiO-66-NH_2. An average crystal size of the synthesized MOF was 150 nm, but most of the crystals formed aggregates due to strong interactions between –COOH and –NH_2 groups remaining on the surface. The octahedral crystal shape of the UiO-66 family was clearly observable in the TEM image. All crystals of Pd@UiO-66-NH_2 had a nanoparticle free region near the surface, which indicated the encapsulation of PdNPs inside the MOF. Smaller MOF crystals with 50~100 nm size were found in the Pd@UiO-66-NH_2 samples and none of the small MOFs contained palladium nanoparticles. Those crystals were supposed to be created at the early stage of the synthesis, before hydrogen gas was injected. The TEM image of Pd containing UiO-66-NH_2 fabricated by the impregnation method is shown in **Figure 7(d)** for comparison. Major parts of the PdNPs are located near/on the surface. Seventy five palladium nanoparticles were sampled

from each introducing method and their diameters were measured (**Figure 8**). Average diameters were 10.96 nm for in situ hydrogen reduction and 4.78 nm for impregnation. Exceptionally large aggregated particles were observed from the impregnation sample. The palladium content of the MOF was 2.74 wt% when measured by the SEM EDS (**Figure 9**).

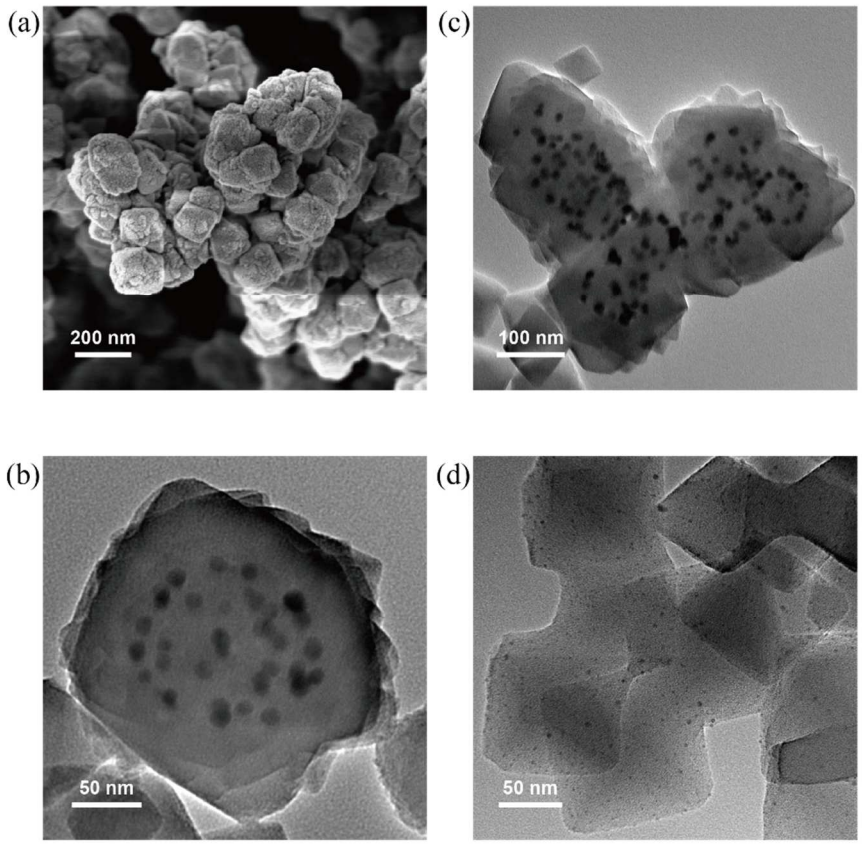

Figure 7 SEM (a) and TEM images (b, c) of Pd@UiO-66-NH_2 and TEM image of Pd introduced UiO-66-NH_2 by impregnation (d).

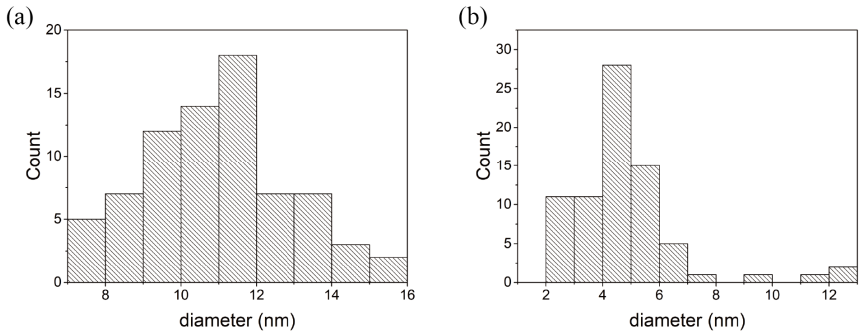

Figure 8 Particle size distribution of Pd encapsulated MOFs. (a) by in situ hydrogen reduction (b) by impregnation.

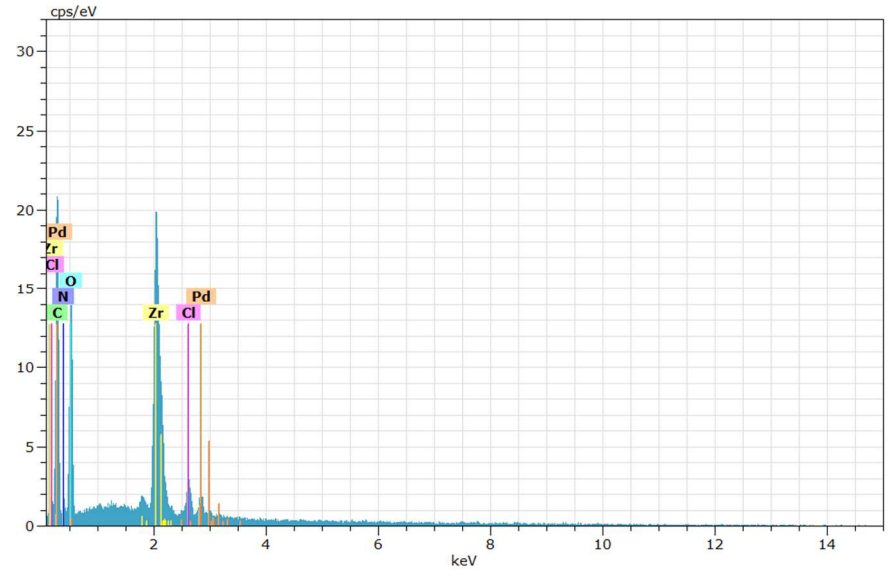

Figure 9 SEM EDS spectrum of Pd@UiO-66-NH_2.

Crystal structures of UiO-66-NH_2 and Pd@UiO-66-NH_2 were investigated by XRD measurements (**Figure 10**). The positions of all characteristic peaks from UiO-66-NH_2 and Pd@UiO-66-NH_2 were well matched and similar to the reported data of UiO-66-NH_2.[35] The characteristic XRD peaks of palladium at 2θ = 40 and 47 degree were not observed probably due to the small particle size.

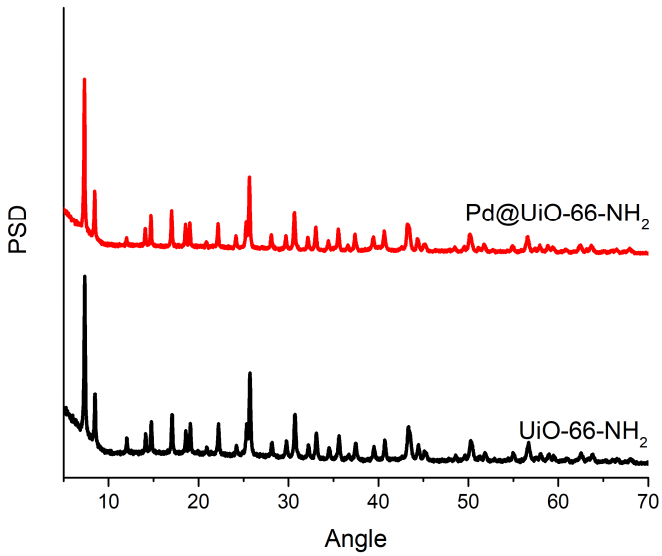

Figure 10 XRD patterns of Pd@UiO-66-NH_2 and UiO-66-NH_2

3.3. Postsynthetic modification of the MOF

Polymerizable vinyl groups were introduced to the MOF by the reaction of an amino group from the organic linker and acryloyl chloride (**Figure 11**). The PSM process did not destroy the crystal structure of the MOF, which was confirmed by the XRD and nitrogen adsorption/desorption measurements (**Figure 12** and **Figure 13**). No major changes were observed in the XRD patterns, adsorption/desorption isotherms, and NLDFT pore size distributions. The surface area of the modified MOF was 829 m^2/g, which decreased by 15.2 % from 978 m^2/g of the unmodified MOF. The modification of aminoterephthalic acid with acryloyl chloride increased molecular weights of the organic linker and the MOF and the surface area decrement after the PSM process was attributable by this weight increase of the MOF.

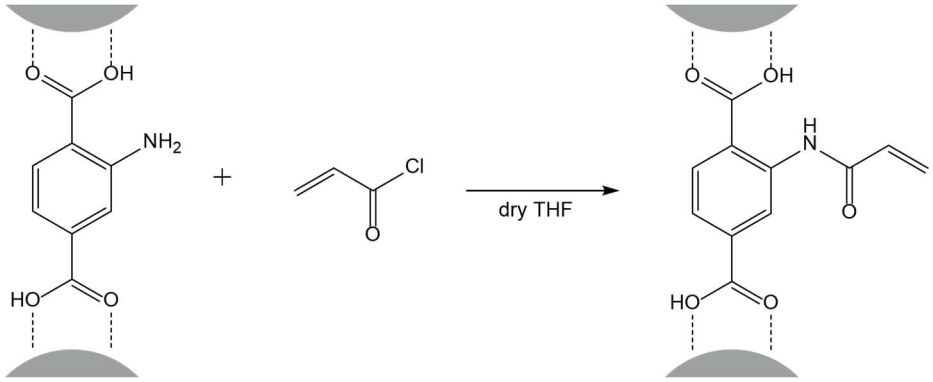

Figure 11 Postsynthetic modification of Pd@UiO-66-NH_2 with acryloyl chloride.

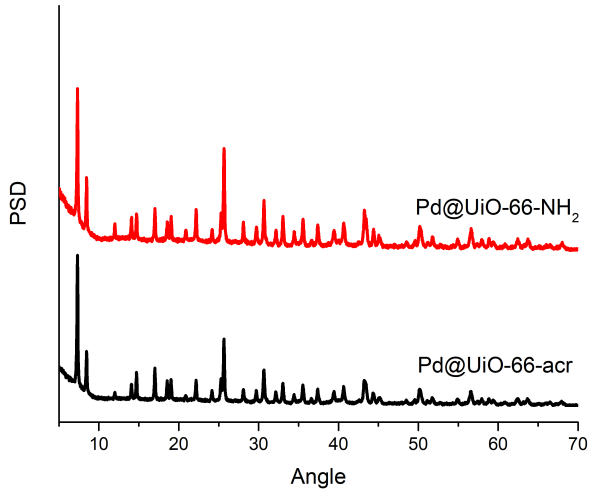

Figure 12 XRD pattern of Pd encapsulated MOF before and after modification.

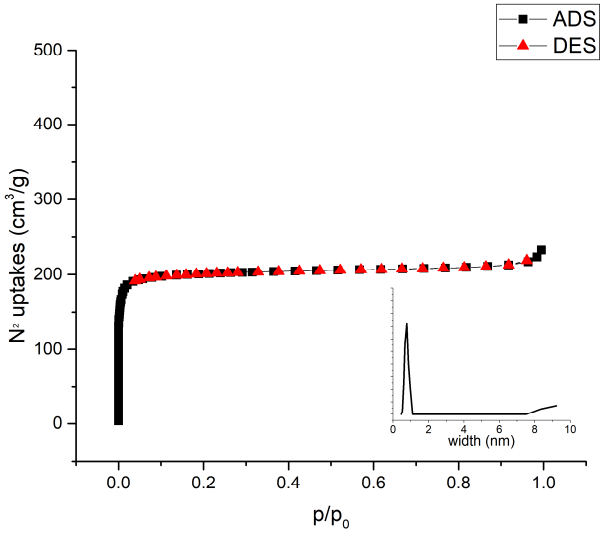

Figure 13 N_2 adsorption/desorption isotherm of Pd@UiO-66-acr. Inset graph is NLDFT pore size distribution.

Unmodified MOF and modified MOF were digested by hydrofluoric acid in d_6-DMSO and used for the NMR measurement (**Figure 14**). Newly appeared peaks at 5.8 ~ 6.5 ppm corresponded to the hydrogens of grafted acryl group. Two sets of aromatic hydrogen peaks (* marked peaks in **Figure 14**) from aminoterephthalic acid were observed due to the protonation of amino groups caused by hydrofluoric acid. The modification ratio was calculated from the peak areas of vinyl hydrogens (6) and aromatic hydrogens (2 + 2*) to be 96.1 %. From the computed ratio and molecular weight increment by the PSM, the

expected surface area of the modified MOF was 801 m^2/g, which was well matched to the measured value.

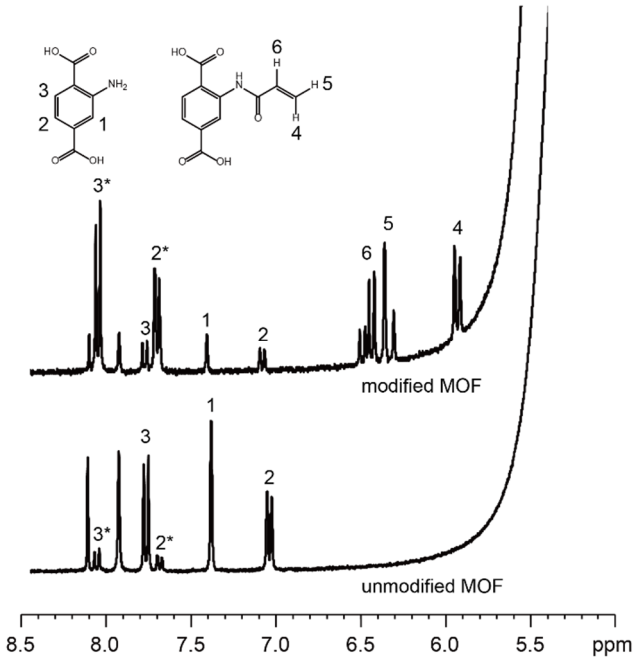

Figure 14 ^{1}H-NMR spectra of digested sample from modified and unmodified MOF. 2* and 3* are correspond to hydrogens from the protonated linker.

3.4. Fabrication of the catalytic hydrogel system

The catalytic hydrogel was prepared by copolymerization of acrylamide and Pd@UiO-66-acr (**Figure 15**). Acrylamide and Pd@UiO-66-acr (15 wt% to acrylamide) were polymerized in the presence of potassium persulfate as an initiator, TEMED as a catalyst, and a small amount of MBAA as a chemical crosslinker in water. The resulting hydrogel showed grey color without any deposition of the MOF (**Figure 16**). The microstructure of the hydrogel was investigated with SEM (**Figure 17**). The hydrogel was freeze-dried for the SEM study. MOF clusters of 300~500 nm sizes were uniformly distributed throughout the hydrogel and no micron sized aggregates were observed. The MOF should be dispersed homogeneously for successful reinforcement of the hydrogel and stable catalytic ability. Both macroscopic and microscopic observation confirmed the homogeneity of the fabricated hydrogel.

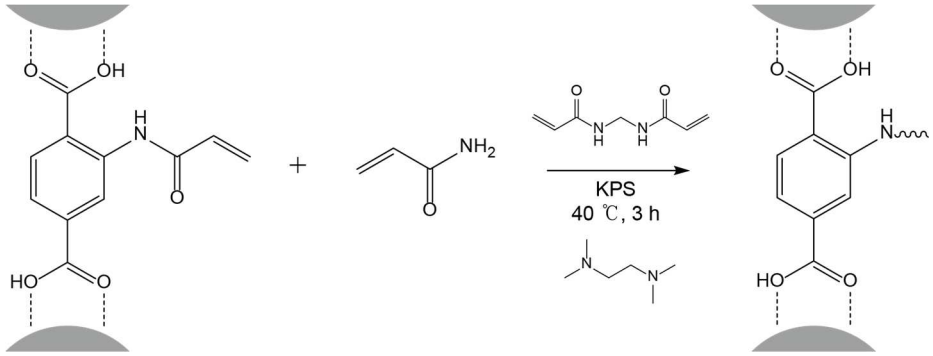

Figure 15 Copolymerization of acrylamide and Pd@UiO-66-acr.

Figure 16 Photographs of the catalytic hydrogel system.

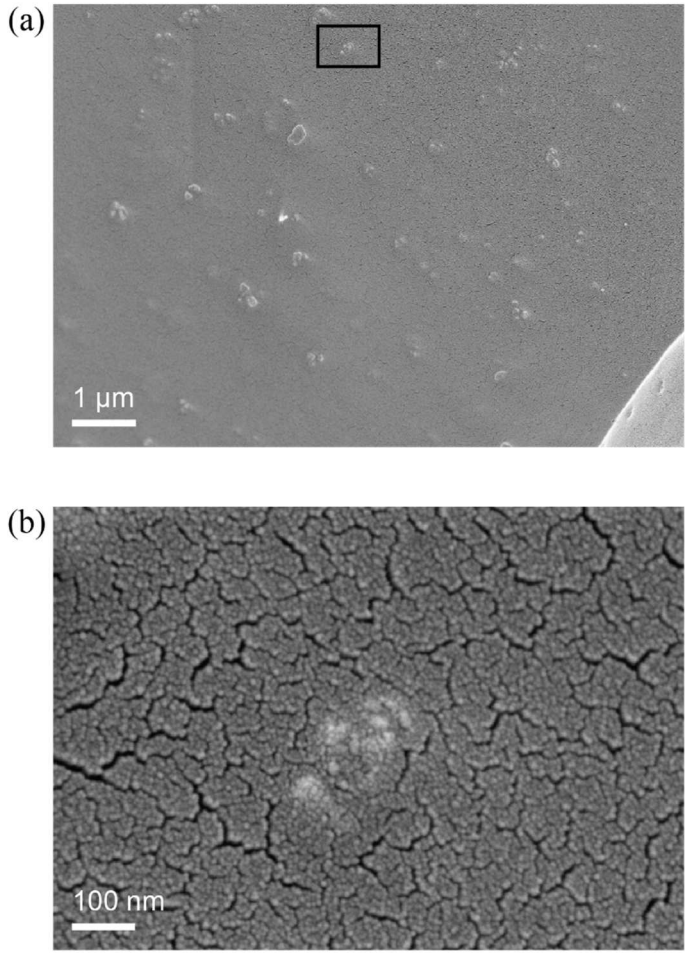

Figure 17 SEM images of the freeze-dried catalytic hydrogel. The area inside of the box in (a) is magnified in (b).

The mechanical properties of the pure acrylamide hydrogel (**AAm gel**), unmodified MOF-hydrogel composite (**unmod gel**), and modified MOF

hydrogel composite (**mod gel**) were investigated by tensile tests (**Figure 18**, **Table 1**). AAm gel had a sticky surface, indicating the low crosslinking density, while unmod gel and mod gel did not show such stickiness. Unmod gel showed 73.7 % higher Young's modulus and 56 % higher elongation than AAm gel. The improvement of the mechanical properties was due to the physical interactions between polyacrylamide chains and the MOF because unmodified MOF did not have copolymerizable vinyl groups. Polyacrylamide chains had a lot of carbonyl groups and amino groups that could interact with the MOF *via* hydrogen bonding. Moreover, anionic sulfate groups at the chain ends originated from initiator species could provide strong interactions with carboxyl groups or exposed metal cores of the MOF. The modulus of mod gel increased by 18.0 % and elongation decreased by 19.3 % compared to those of unmod gel. The increased modulus and lower stretchability resulted from the increase in chemical crosslinking density. These results suggested that the modified MOF could act as a double crosslinker, which could participate in both chemical crosslinking and physical crosslinking.

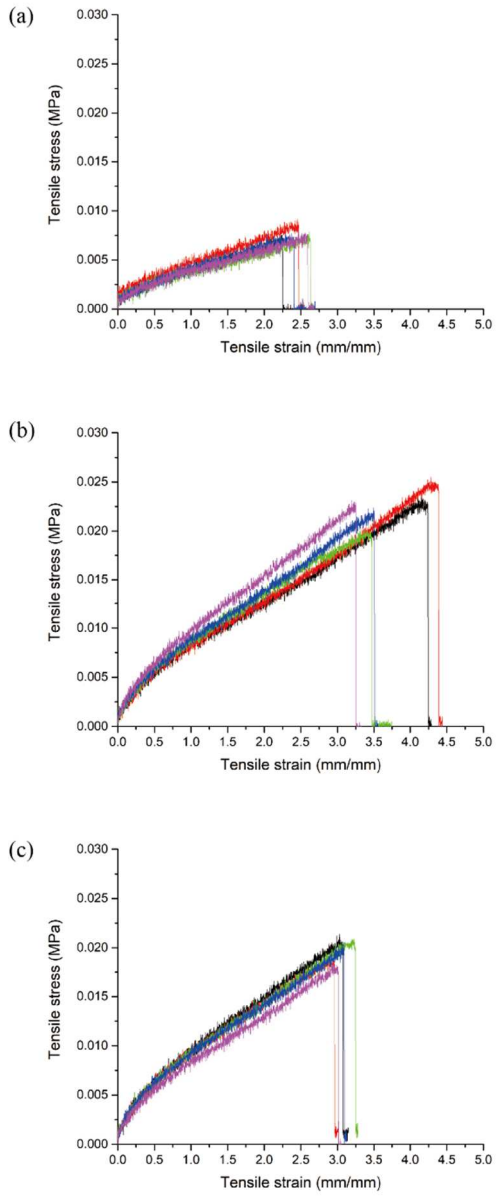

Figure 18 Tensile test results of (a) pure acrylamide hydrogel, (b) unmodified MOF-hydrogel composite, and (c) modified MOF-hydrogel composite.

Table 1 Mechanical properties of prepared hydrogels.

	AAm gel	**unmod gel**	**mod gel**
Modulus(kPa)	6.488	11.27	13.30
Elongation at break(%)	248.2	387.2	312.3

3.5. Suzuki-Miyaura coupling reaction

According to Hoffman, water in hydrogels is classified into two types, bounded water that directly interacts with polymer chains and free water that fills the space between the chains by osmotic driving force to dilute network chains.[36] Bounded water cannot solvate and dissolve other molecules, while free water can interact with external solutions and absorb solutes. The reaction in a hydrogel occurs by contact of absorbed reactant molecules in free water with palladium encapsulated MOF crystals within the network. Because water was incapable of dissolving iodobezene, ethanol/water was chosen as a reaction solvent.

The Suzuki-Miyaura coupling reaction was carried out to evaluate the catalytic ability of the fabricated hydrogel system (**Figure 19**). A 750 mg of sheet-formed wet catalyst (contains 0.002 mmol Pd) was added to a solution of iodobenzene (0.25 mmol), phenylboronic acid (0.3 mmol), and potassium carbonate (0.5mmol) in 2 ml of aqueous ethanol (1:1 v/v). The reaction vessel was heated to 60 ℃ with stirring and kept for 24 h. The product was collected

by extraction with ethyl acetate and analyzed by ^{1}H-NMR spectroscopy (**Figure 20**). Yield calculated by the peak area ratio of biphenyl and iodobenzene,[37] was 94 %.

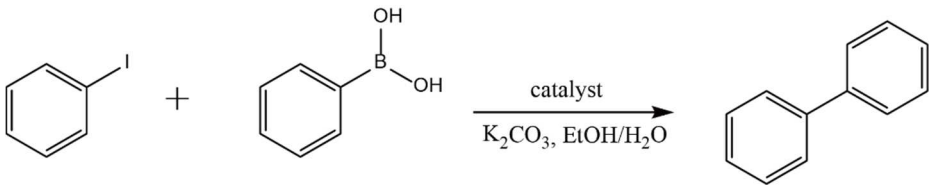

Figure 19 Suzuki-Miyaura coupling reaction with catalytic hydrogel system.

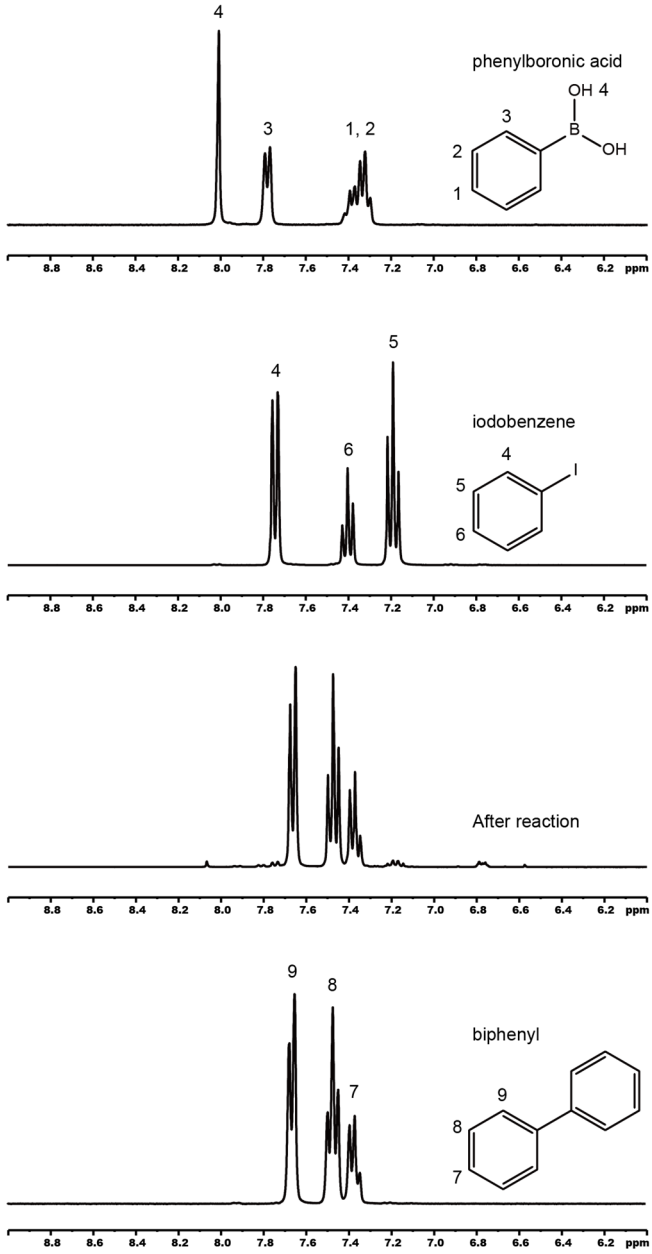

Figure 20 ^{1}H-NMR spectra of phenylboronic acid, iodobenzene, reaction mixture after 24 h at 60 °C, and biphenyl in d_6-DMSO.

The role of MOF as a catalyst cage was investigated by the recycle test. The hydrogel catalyst was simply recovered from the reaction mixture and washed with ethyl acetate for reuse. The coupling reaction was performed under same conditions and no significant loss of catalytic ability was observed until 5 cycles. The hydrogel maintained its morphology even after a number of reaction cycles at elevated temperatures and stirring.

4. Conclusion

We fabricated a new catalytic hydrogel system with PdNPs containing MOFs. Palladium nanoparticles were encapsulated in UiO-66-NH_2 by the in situ hydrogen reduction method. No surface aggregation of the nanoparticles was observed. Postsynthetic modification (PSM) of amino groups on the organic linkers with acryloyl chloride allowed us to introduce polymerizable vinyl moieties to the MOF. Successful modification without any damage on the MOF structure was confirmed by nuclear magnetic resonance spectra, nitrogen adsorption/desorption isotherms, and X-ray diffraction patterns. The catalytic hydrogen system was fabricated by free radical polymerization of acrylamide, modified MOFs and a small amount of chemical crosslinker. The MOF clusters were uniformly dispersed in the hydrogel. The tensile test revealed that a modified MOF acted as a dual crosslinker to form the chemically and physically crosslinked hydrogel. We carried out Suzuki-Miyaura coupling reaction to evaluate the catalytic ability of the catalytic hydrogel system. The reaction was completed with a good yield. The catalytic hydrogel could be easily recovered and recycled.

5. References

1. Lipshutz, B. H.; Gallou, F.; Handa, S. *ACS Sustain. Chem. Eng.* **2016**, *4*, 5838–5849.
2. Miyaura, N.; Yamada, K.; Suginome, H.; Suzuki, A. *J. Am. Chem. Soc.* **1985**, *107*, 972–980.
3. Butun, S.; Sahiner, N. *Polymer (Guildf).* **2011**, *52*, 4834–4840.
4. Lee, Y.; Hong, M. C.; Ahn, H.; Yu, J.; Rhee, H. *J. Organomet. Chem.* **2014**, *769*, 80–93.
5. Maity, M.; Maitra, U. *J. Mater. Chem. A* **2014**, *2*, 18952–18958.
6. Firouzabadi, H.; Iranpoor, N.; Gholinejad, M.; Kazemi, F. *RSC Adv.* **2011**, *1*, 1013–1019.
7. Stefanescu, E. A.; Stefanescu, C.; Daly, W. H.; Schmidt, G.; Negulescu, I. I. *Polymer (Guildf).* **2008**, *49*, 3785–3794.
8. Haraguchi, K. *Colloid Polym. Sci.* **2011**, *289*, 455–473.
9. Gu, Z. Y.; Yan, X. P. *Angew. Chemie - Int. Ed.* **2010**, *49*, 1477–1480.
10. Maes, M.; Alaerts, L.; Vermoortele, F.; Ameloot, R.; Couck, S.; Finsy, V.; Denayer, J. F. M.; De Vos, D. E. *J. Am. Chem. Soc.* **2010**, *132*, 2284–2292.
11. Wang, C.; Liu, X.; Chen, J. P.; Li, K. *Sci. Rep.* **2015**, *5*, 1–10.
12. Taylor-Pashow, K. M. L.; Della Rocca, J.; Xie, Z.; Tran, S.; Lin, W. *J. Am. Chem. Soc.* **2009**, *131*, 14261–14263.

13. Alkordi, M. H.; Liu, Y.; Larsen, R. W.; Eubank, J. F.; Eddaoudi, M. *J. Am. Chem. Soc.* **2008**, *130*, 12639–12641.
14. Jiang, H.; Liu, B.; Akita, T.; Haruta, M.; Sakurai, H.; V, K. U.; Ku, N. *J. Am. Chem. Soc.* **2009**, *131*, 11302–11303.
15. Dong, W.; Feng, C.; Zhang, L.; Shang, N.; Gao, S.; Wang, C.; Wang, Z. *Catal. Letters* **2016**, *146*, 117–125.
16. Pourkhosravani, M.; Dehghanpour, S.; Farzaneh, F. *Catal. Letters* **2016**, *146*, 499–508.
17. Sun, D.; Li, Z. *J. Phys. Chem. C* **2016**, *120*, 19744–19750.
18. Liu, H.; Chang, L.; Bai, C.; Chen, L.; Luque, R.; Li, Y. *Angew. Chemie - Int. Ed.* **2016**, *55*, 5019–5023.
19. Hu, Z.; Zhang, K.; Zhang, M.; Guo, Z.; Jiang, J.; Zhao, D. *ChemSusChem* **2015**, *7*, 2791–2795.
20. Savonnet, M.; Aguado, S.; Ravon, U.; Bazer-Bachi, D.; Lecocq, V.; Bats, N.; Pinel, C.; Farrusseng, D. *Green Chem.* **2009**, *11*, 1729–1732.
21. Prasetya, N.; Ladewig, B. P. *Sci. Rep.* **2017**, *7*, 1–6.
22. Venna, S. R.; Lartey, M.; Li, T.; Spore, A.; Kumar, S.; Nulwala, H. B.; Luebke, D. R.; Rosi, N. L.; Albenze, E. *J. Mater. Chem. A* **2015**, *3*, 5014–5022.
23. Sarker, M.; Song, J. Y.; Jhung, S. H. *Chem. Eng. J.* **2018**, *331*, 124–131.
24. Zhang, Y.; Feng, X.; Li, H.; Chen, Y.; Zhao, J.; Wang, S.; Wang, L.; Wang, B. *Angew. Chemie - Int. Ed.* **2015**, *54*, 4259–4263.
25. Zhang, G.; Li, J.; Wang, N.; Fan, H.; Zhang, R.; Zhang, G.; Ji, S. *J. Memb. Sci.* **2015**, *492*, 322–330.

26. Ahmadi Feijani, E.; Tavasoli, A.; Mahdavi, H. *Ind. Eng. Chem. Res.* **2015**, *54*, 12124–12134.
27. Shen, J.; Liu, G.; Huang, K.; Li, Q.; Guan, K.; Li, Y.; Jin, W. *J. Memb. Sci.* **2016**, *513*, 155–165.
28. Ananthoji, R.; Eubank, J. F.; Nouar, F.; Mouttaki, H.; Eddaoudi, M.; Harmon, J. P. *J. Mater. Chem.* **2011**, *21*, 9587–9594.
29. Xiao, J.; Chen, S.; Yi, J.; Zhang, H. F.; Ameer, G. A. *Adv. Funct. Mater.* **2017**, *27*.
30. Garai, A.; Shepherd, W.; Huo, J.; Bradshaw, D. *J. Mater. Chem. B* **2013**, *1*, 3678–3684.
31. Zhu, H.; Zhang, Q.; Zhu, S. *ACS Appl. Mater. Interfaces* **2016**, *8*, 17395–17401.
32. Leus, K.; Bogaerts, T.; De Decker, J.; Depauw, H.; Hendrickx, K.; Vrielinck, H.; Van Speybroeck, V.; Van Der Voort, P. *Microporous Mesoporous Mater.* **2016**, *226*, 110–116.
33. Xie, K.; Fu, Q.; He, Y.; Kim, J.; Goh, S. J.; Nam, E.; Qiao, G. G.; Webley, P. A. *Chem. Commun.* **2015**, *51*, 15566–15569.
34. Sindoro, M.; Yanai, N.; Jee, A. Y.; Granick, S. *Acc. Chem. Res.* **2014**, *47*, 459–469.
35. Liu, W.; Huang, J.; Yang, Q.; Wang, S.; Sun, X.; Zhang, W.; Liu, J.; Huo, F. *Angew. Chemie - Int. Ed.* **2017**, *56*, 5512–5516.
36. Hoffman. *Adv. Drug Deliv. Rev.* **2012**, *64*, 18–23.
37. Badone, D.; Baroni, M.; Cardamone, R.; Ielmini, A.; Guzzi, U. *J. Org. Chem.* **1997**, *62*, 7170–7173.

국문 요약

환경오염 문제가 점점 대두되면서 휘발성 유기용매의 사용을 감소시킬 수 있는 수용액에서의 화학반응이 주목을 받고 있다. 본 연구에서는 물을 용매로 하는 스즈키-미야우라 반응에 적합한 하이드로젤 촉매를 제조하였다. 팔라듐 나노입자를 도입한 금속-유기 구조체(MOF)를 개질한 후 하이드로젤 제조에 이용하여 기계적 특성과 촉매 활성이 우수한 촉매 시스템을 얻었다. MOF 로는 2-aminoterephthalic acid 와 zirconium(IV) chloride 로부터 합성한 UiO-66-NH_2 를 이용하였다. 수소 기체를 이용하여 팔라듐 나노입자를 UiO-66-NH_2 안에서 생성하고 비닐기를 UiO-66-NH_2 에 도입하였다. 비닐기가 도입된 MOF 와 아크릴아마이드의 라디칼 중합반응을 소량의 가교제 존재 하에 수행하여 하이드로젤 촉매를 제조하였다. 하이드로젤 촉매의 촉매 활성 및 재사용 가능성을 phenylboronic acid 와 iodobenzene 의 스즈키-미야우라 반응을 물-에탄올 용매에서 수행하여 조사하였다.

주요어: 하이드로젤 촉매, 비균질 촉매, 팔라듐 나노입자, 스즈키-미야우라 반응, 수용액 반응